

## Optical properties of GaN wurtzite quantum wires

This article has been downloaded from IOPscience. Please scroll down to see the full text article.

2006 J. Phys.: Condens. Matter 18 3107

(<http://iopscience.iop.org/0953-8984/18/11/016>)

View [the table of contents for this issue](#), or go to the [journal homepage](#) for more

Download details:

IP Address: 129.252.86.83

The article was downloaded on 28/05/2010 at 09:08

Please note that [terms and conditions apply](#).

# Optical properties of GaN wurtzite quantum wires

X W Zhang and J B Xia

Chinese Center of Advanced Science and Technology (World Laboratory), Beijing 100080,  
People's Republic of China

and

Institute of Semiconductors, Chinese Academy of Sciences, Beijing 100083,  
People's Republic of China

Received 11 October 2005, in final form 13 February 2006

Published 1 March 2006

Online at [stacks.iop.org/JPhysCM/18/3107](http://stacks.iop.org/JPhysCM/18/3107)

## Abstract

The electronic structure and optical properties of freestanding GaN wurtzite quantum wires are studied in the framework of six-band effective-mass envelope function theory. It is found that the electron states are either twofold or fourfold degenerate. There is a dark exciton effect when the radius  $R$  of GaN wurtzite quantum wires is in the range of [0.7, 10.9] nm. The linear polarization factors are calculated in three cases, the quantum confinement effect (finite long wire), the dielectric effect and both effects (infinitely long wire). It is found that the linear polarization factor of a finite long wire whose length is much less than the electromagnetic wavelength decreases as  $R$  increases, is very close to unity (0.979) at  $R = 1$  nm, and changes from a positive value to a negative value around  $R = 4.1$  nm. The linear polarization factor of the dielectric effect is 0.934, independent of radius, as long as the radius remains much less than the electromagnetic wavelength. The result for the two effects shows that the quantum confinement effect gives a correction to the dielectric effect result. It is found that the linear polarization factor of very long (treated approximately as infinitely long) quantum wires is in the range of [0.8, 1]. The linear polarization factors of the quantum confinement effect of CdSe wurtzite quantum wires are calculated for comparison. In the CdSe case, the linear polarization factor of  $R = 1$  nm is 0.857, in agreement with the experimental results (Hu *et al* 2001 *Science* **292** 2060). This value is much smaller than unity, unlike 0.979 in the GaN case, mainly due to the big spin–orbit splitting energy  $\Delta_{\text{so}}$  of CdSe material with wurtzite structure.

## 1. Introduction

Low dimensional systems such as semiconductor quantum dots and quantum wires have fascinating and technologically useful optical and electric properties. Studies on these systems advance our knowledge of low dimensional physics and chemistry. Semiconductor quantum wires exhibit novel electric and optical properties owing to their unique structural one-dimensionality and possible quantum confinement effects in two dimensions. Quantum wires

**Table 1.** GaN effective-mass parameters of hole.

$L$	$M$	$N$	$R$	$S$	$T$	$Q$
6.3055	0.1956	0.3813	6.1227	0.4335	7.3308	4.0200

have been evaluated for potential applications as lasers [1–3], light-emitting diodes [4, 5], and photodetectors [6, 7].

Nowadays, the method to synthesize quantum wires has been improved. GaN wurtzite quantum wires in a large range of radius are synthesized by different methods [8–14], whose photoluminescence [15] is measured. High quality ultra-fine GaN nanowires are synthesized [16]. Recently much attention has been paid to the linear polarized optical property of quantum wires. Linear polarized emissions from quantum wires are observed [17–21], and explained by the dielectric effect [22] or the quantum confinement effect [23, 24]. Actually, wurtzite single-crystal bulk material [25] also has linear polarized emissions.

The electronic structures of nanowires with zinc-blende structure have been studied in the framework of the six-band effective-mass approximation [26]. In this paper, we apply the formal model to investigate optical properties of wurtzite quantum wires. The remainder of this paper is organized as follows. In section 2 we give the form of the Hamiltonian. Our numerical results and discussions are given in section 3. Finally, we draw a brief conclusion in section 4.

## 2. Model and calculation

The hole effective-mass Hamiltonian for wurtzite semiconductors in the case of zero spin-orbital coupling is given by [27]

$$H_{h0} = \frac{1}{2m_0} \begin{vmatrix} Lp_x^2 + Mp_y^2 + Np_z^2 & Rp_xp_y & Qp_xp_z \\ Rp_xp_y & Lp_y^2 + Mp_x^2 + Np_z^2 & Qp_y p_z \\ Qp_xp_z & Qp_y p_z & S(p_x^2 + p_y^2) + Tp_z^2 + 2m_0\Delta_c \end{vmatrix}, \quad (1)$$

where the valence band basic functions are  $X$ -like,  $Y$ -like ( $\Gamma_6$ ) and  $Z$ -like ( $\Gamma_1$ ) functions, respectively;  $L, M, \dots, S, T$  are effective-mass parameters. Hereafter, we take the negative hole energy as positive. The effective-mass parameters of GaN in Hamiltonian (1) are shown in table 1 [27].

We consider a cylinder with radius  $R$ , and assume that the cylinder has a sharp boundary, so that the wavefunctions at the boundary are zero. In order to calculate in the cylindrical coordinate, we transform the hole Hamiltonian (1) from the basic functions  $X, Y$ , and  $Z$  to the  $1/\sqrt{2}(X + iY)$ ,  $1/\sqrt{2}(X - iY)$ , and  $Z$ ,

$$H_{h0} = \frac{1}{2m_0} \begin{vmatrix} P_1 & F & G \\ F^* & P_1 & G^* \\ G^* & G & P_3 \end{vmatrix}, \quad (2)$$

where

$$\begin{aligned} P_1 &= \frac{L + M}{2} p_- p_+ + Np_z^2, \\ P_3 &= Sp_- p_+ + Tp_z^2 + 2m_0\Delta_c, \\ F &= \frac{L - M - R}{4} p_+^2 + \frac{L - M + R}{4} p_-^2, \\ G &= \frac{1}{\sqrt{2}} Qp_- p_z, \\ p_{\pm} &= p_x \pm ip_y. \end{aligned} \quad (3)$$

The spin-orbital coupling (SOC) Hamiltonian is written as

$$H_{\text{so}} = \begin{pmatrix} 0 & 0 & 0 & 0 & 0 & 0 \\ 0 & 2\lambda & 0 & 0 & 0 & -\sqrt{2}\lambda \\ 0 & 0 & \lambda & \sqrt{2}\lambda & 0 & 0 \\ 0 & 0 & \sqrt{2}\lambda & 2\lambda & 0 & 0 \\ 0 & 0 & 0 & 0 & 0 & 0 \\ 0 & -\sqrt{2}\lambda & 0 & 0 & 0 & \lambda \end{pmatrix}, \quad (4)$$

where

$$\lambda = \frac{\hbar^2}{4m_0^2c^2} \langle X | \frac{\partial V}{\partial x} \frac{\partial}{\partial y} | Y \rangle = \frac{\Delta_{\text{so}}}{3}. \quad (5)$$

Here, we take the basic functions as  $1/\sqrt{2}(X+iY) \uparrow$ ,  $1/\sqrt{2}(X-iY) \uparrow$ ,  $Z \uparrow$ ,  $1/\sqrt{2}(X+iY) \downarrow$ ,  $1/\sqrt{2}(X-iY) \downarrow$  and  $Z \downarrow$ . We make the cylindrical symmetry approximation for the valence bands, i.e. assume that the coefficient of the  $p_+^2$  term in  $F$  of equation (3) is zero,  $L - M - R = 0$ , which is verified from table 1.

In the cylindrical symmetry approximation, we expand the wavefunction of the hole state in Bessel functions,

$$\phi_{J,k} = \sum_n \begin{pmatrix} b_{L-1,k,n,\uparrow} A_{L-1,n} J_{L-1}(k_n^{L-1} r) e^{i(L-1)\theta} \\ c_{L+1,k,n,\uparrow} A_{L+1,n} J_{L+1}(k_n^{L+1} r) e^{i(L+1)\theta} \\ d_{L,k,n,\uparrow} A_{L,n} J_L(k_n^L r) e^{iL\theta} \\ b_{L,k,n,\downarrow} A_{L,n} J_L(k_n^L r) e^{iL\theta} \\ c_{L+2,k,n,\downarrow} A_{L+2,n} J_{L+2}(k_n^{L+2} r) e^{i(L+2)\theta} \\ d_{L+1,k,n,\downarrow} A_{L+1,n} J_{L+1}(k_n^{L+1} r) e^{i(L+1)\theta} \end{pmatrix} e^{ikz}, \quad (6)$$

where  $J = L + 1/2$  is the total azimuthal angular momentum, and  $A_{L,n}$  is the normalization constant,

$$A_{L,n} = \frac{1}{\sqrt{\pi} R J_{L+1}(\alpha_n^L)}. \quad (7)$$

$\alpha_n^L = k_n^L R$  is the  $n$ th zero point of the Bessel function  $J_L(x)$ ,  $R$  is the radius of the cylinder, and  $k$  is the wavevector along the  $z$  direction. In the cylindrical symmetry, the system has the conserved quantum number  $k$  and  $J$ , the total azimuthal angular momentum. Therefore the summation in equation (6) is only over  $n$ . In calculating the matrix elements of the Hamiltonian equation (2) we can use the property of the operators  $p_{\pm}$ ,

$$p_{\pm} J_L(k_n^L r) e^{iL\theta} = \mp \frac{\hbar}{i} k_n^L J_{L\pm 1}(k_n^L r) e^{i(L\pm 1)\theta}. \quad (8)$$

The electron Hamiltonian is

$$H_{e0} = \frac{1}{2m_x^*} p_- p_+ + \frac{1}{2m_z^*} p_z^2. \quad (9)$$

We take the basic functions as  $S \uparrow$  and  $S \downarrow$ ;  $S$  is the Bloch state of the conduction-band bottom. The wavefunction of the electron state is expanded in Bessel functions,

$$\phi_{J,k}^e = \sum_n \begin{pmatrix} e_{L,k,n,\uparrow} A_{L,n} J_L(k_n^L r) e^{iL\theta} \\ e_{L+1,k,n,\downarrow} A_{L+1,n} J_{L+1}(k_n^{L+1} r) e^{i(L+1)\theta} \end{pmatrix} e^{ikz}. \quad (10)$$

We also calculate the linear polarization factor of the wires, and assume that the light wave propagates along the  $y$  direction. The linear polarization factor is affected by the quantum confinement effect and the dielectric effect. Taking into account only the quantum confinement

effect, with the optical transition between a given electron state and a given hole state, the intensities of  $z$  and  $x$  polarized transitions are proportional to

$$I_z = \left\{ \sum_{L,k,n,s} d_{L,k,n,s} e_{L,k,n,s} \right\}^2, \quad (11)$$

$$I_x = \left\{ \sum_{L,k,n,s} (b_{L,k,n,s} e_{L,k,n,s} + c_{L,k,n,s} e_{L,k,n,s}) / \sqrt{2} \right\}^2, \quad (12)$$

where  $s$  denotes spin-up  $\uparrow$  or spin-down  $\downarrow$ , and  $b_{L,k,n,s}$ ,  $c_{L,k,n,s}$ ,  $d_{L,k,n,s}$  and  $e_{L,k,n,s}$  are given in equations (6) and (10), respectively.

For the wires, the dielectric effect vanishes in the  $z$  direction, but remains in the perpendicular directions. Due to the dielectric effect only, the proportion of the intensity of the  $z$  polarized transition to the intensity of the  $x$  polarized transition is given by [22]

$$W = \frac{I'_z}{I'_x} = \frac{(\varepsilon_{\text{GaN}} + \varepsilon_0)^2 + 2\varepsilon_0^2}{6\varepsilon_0^2}, \quad (13)$$

where  $\varepsilon_{\text{GaN}}$  and  $\varepsilon_0$  are the dielectric constants in and outside the wire. Then the linear polarization factor is given by

$$P = (I_z W - I_x) / (I_z W + I_x), \quad (14)$$

where  $I_z$  and  $I_x$  are given by equations (11) and (12). Considering the temperature effect, we multiply each state by the Boltzmann distribution factor, and sum up all contributions to the intensities.

### 3. Results and discussion

We calculated the electronic structure and optical properties of freestanding GaN wurtzite quantum wires. Except the effective-mass parameters in Hamiltonian (1) shown in table 1, other parameters used in this paper are taken as the electron effective masses perpendicular to and along the  $c$  axis,  $m_x^* = 0.22 m_0$  and  $m_z^* = 0.20 m_0$ , respectively, the dielectric constant  $\varepsilon_{\text{GaN}} = 12.2$ , the bandgap  $E_g = 3.4953$  eV, the crystal field splitting energy  $\Delta_c = 0.021$  eV and the spin-orbit splitting energy  $\Delta_{\text{so}} = 0.018$  eV [28]. The unit of energy is

$$\varepsilon_0 = \frac{1}{2m_0} \left( \frac{\hbar}{R} \right)^2. \quad (15)$$

#### 3.1. Electronic structure

The electron states (all  $J$ ) of GaN wurtzite quantum wire as functions of  $k$  are shown in figure 1. The symbol of each energy level represents the main components of its wavefunction. For example,  $(1, 0)S \uparrow$  means that the state consists mainly of the  $n = 1$ ,  $L = 0$  state of the effective-mass envelope function multiplied by the  $S$  Bloch state of the conduction-band bottom and the spin-up state. As we use the energy unit  $\varepsilon_0$  and  $k$  unit  $\pi/R$ , the energy levels of the electron are independent of  $R$ . We see that the electron states are degenerate. For  $L = 0$ , they are twofold degenerate with spin-up and spin-down states. For  $L \neq 0$ , they are fourfold degenerate with  $\pm L$  and spin-up, spin-down states. The energy levels increase with increasing  $k$  as quadratic terms of  $k$ , due to the quadratic terms of  $p_z$  in equation (3). The hole states of GaN wurtzite quantum wire with radius of  $R = 2.0$  nm and  $J = 1/2$  as functions of  $k$  are shown in figure 2. The hole states of GaN wurtzite quantum wire with radius of  $R = 2.0$  nm and  $J = 3/2$  as functions of  $k$  are shown in figure 3. The symbol of each energy level represents the

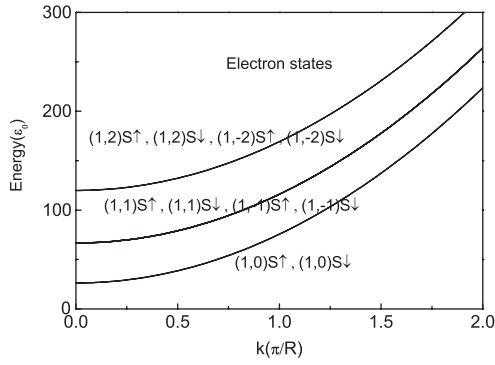


**Figure 1.** Electron states (all  $J$ ) of GaN wurtzite quantum wire as functions of  $k$ .

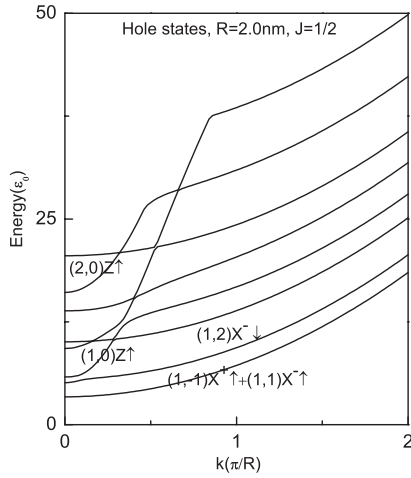


**Figure 2.** Hole states of GaN wurtzite quantum wire with radius of  $R = 2.0$  nm and  $J = 1/2$  as functions of  $k$ .

main components of its wavefunction. For example,  $(1, 0)X^+ \uparrow$  means that the state consists mainly of the  $n = 1$ ,  $L = 0$  state of the effective-mass envelope function multiplied with the  $1/\sqrt{2}(X + iY)$  Bloch state of the valence-band top and the spin-up state. We see that the energy levels increase as  $k$  increases. The levels of the states with  $Z$  Bloch state of the valence-band top increase more quickly than the levels of the states with  $1/\sqrt{2}(X + iY)$  and  $1/\sqrt{2}(X - iY)$  Bloch states. This is because the coefficients of the  $p_z^2$  terms in equation (3) of the two kinds of basic state  $Z$  and  $X, Y$  are different,  $T$  and  $N$ , respectively, and  $T$  is much greater than  $N$  as shown in table 1.

The hole states ( $J > 0$ ) of GaN wurtzite quantum wires at  $k = 0$  as functions of  $R$  are shown in figure 4. Because the energies of valence-band states increase with increasing  $k$  (see figures 2 and 3), the lowest state at  $k = 0$  in figure 4 is the ground state of the valence band. We see that the wavefunction of the ground state changes as  $R$  increases. When  $R$  is smaller than 0.7 nm, the ground state is  $(1, 0)Z \uparrow$ , a state with  $Z$  Bloch state, due to the quantum confinement effect. When  $R$  is bigger than 10.9 nm, the ground state is  $(1, 0)X^+ \uparrow$ , a state with  $1/\sqrt{2}(X + iY)$  Bloch state, due to the crystal field splitting energy. When  $R$  is in the range of [0.7, 10.9] nm, the ground state is  $(1, -1)X^+ \uparrow + (1, 1)X^- \uparrow$ , a state with  $L = \pm 1$ , which is different from  $L = 0$  of the ground state of the conduction band. At low temperature, the electron and hole distribute in the ground state of the conduction band and the ground state of the valence band, respectively. So when  $R$  is in the range of [0.7, 10.9] nm, the electron and hole cannot be recombined directly, that means that there is a dark exciton effect.

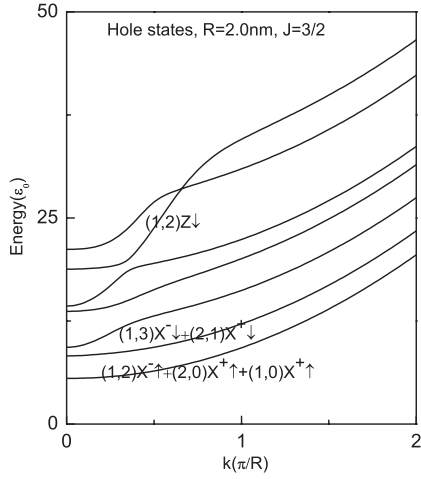


**Figure 3.** Hole states of GaN wurtzite quantum wire with radius of  $R = 2.0$  nm and  $J = 3/2$  as functions of  $k$ .

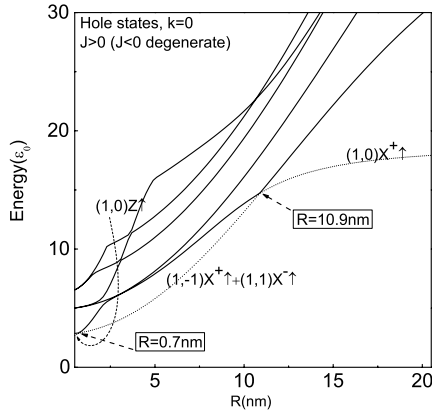


**Figure 4.** Hole states ( $J > 0$ ) of GaN wurtzite quantum wires with  $k = 0$  as functions of  $R$ .

### 3.2. Linear polarization

The calculated linear polarization factors of GaN wurtzite quantum wires ignoring the dielectric effect as functions of  $R$  are shown in figure 5(a). We assume that the finite long wire can also be calculated approximately in our infinitely long wire model. The dielectric effect remains in the long axis direction when the length is smaller than 100 nm, less than the electromagnetic wavelength [22]. The dielectric effect remains in the perpendicular directions when the radius is small, that means that the dielectric effect is isotropic, and can be ignored. The solid line is the case at  $T = 300$  K. We see that when  $R = 1$  nm, the linear polarization factor is 0.979, which is very close to unity, due to the strong quantum confinement effect, which makes the state with the  $Z$  Bloch state the lowest state of the valence band, as shown in figure 4. The linear polarization factor decreases as  $R$  increases, and changes from a positive value to a negative value around  $R = 4.1$  nm, because the quantum confinement effect becomes weak with increasing  $R$ . When  $R$  is greater than 4.1 nm, the quantum confinement effect is so weak that it cannot compensate the effect of the crystal field splitting energy  $\Delta_c$ , which makes the  $X$ - $Y$  Bloch state the lowest state of the valence band, as shown in figure 4, similar to the bulk material case. The dotted line is the case at  $T = 100$  K. We see that at lower temperature the linear polarization factor remains a big positive value (nearly unity) at larger radius, and decreases more quickly with increasing  $R$ . The calculated linear polarization factors of GaN

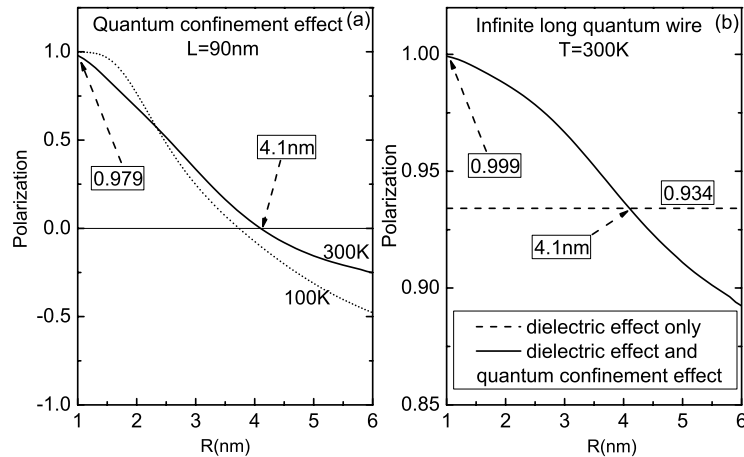


**Figure 5.** (a) Calculated linear polarization factor of GaN wurtzite quantum wires ignoring the dielectric effect as functions of  $R$ . We assume that the finite long wire can also be calculated approximately in our infinite long wire model. We choose the length of wire  $L = 90$  nm and  $L/(2R) \geq 7.5$  so that the dielectric effect can be ignored (isotropic) [22] and the infinite long wire model is also suitable. (b) Calculated linear polarization factor of GaN wurtzite quantum wires taking into account the dielectric effect as functions of  $R$ .

wurtzite quantum wires taking into account the dielectric effect as functions of  $R$  are shown in figure 5(b). We assume that the wires are infinitely long so that the dielectric effect vanishes in the long axis direction, but remains in the perpendicular directions, that means that the dielectric effect is not isotropic, and cannot be ignored. The dielectric constants are  $\epsilon_{\text{GaN}} = 12.2$  [28] in the wire, and  $\epsilon_0 = 1$  in the vacuum. The dashed line shows the result taking into account only the dielectric effect. The linear polarization factor is independent of  $R$ , equal to 0.934, as long as the radius remains much less than the electromagnetic wavelength [22], as we do not take into account the quantum confinement effect in this case. The quantum confinement effect gives a correction to the dielectric effect result (dashed line). The calculated result taking into account both the dielectric effect and the quantum confinement effect is shown by the solid line in figure 5(b). We see that the linear polarization factor of infinitely long (very long, for example, longer than  $1 \mu\text{m}$ , may be treated approximately as infinitely long) quantum wires is in the range of  $[0.8, 1]$ . Experimentally, the linear polarization factor of InP quantum wires was measured to be about 0.95 [29]. This value is very close to our result of the GaN case. As the quantum confinement effect only gives a correction to the dielectric effect result, and the dielectric constants of GaN(12.2) and InP(12.6) [28] are very close, so the linear polarization factors are close too. As shown in figure 5(b), the solid line crosses with the dashed line at  $R = 4.1$  nm, where the linear polarization factor of the quantum confinement effect in figure 5(a) is zero. The linear polarization factor of the quantum confinement effect at  $R = 1$  nm is 0.979. Because this value is very close to unity, the correction of the dielectric effect is very small, from 0.979 to 0.999 28.

The linear polarization factors of the quantum confinement effect of CdSe wurtzite quantum wires are calculated for comparison. The calculated linear polarization factor of CdSe wurtzite quantum wires (long finite) ignoring the dielectric effect as functions of  $R$  are shown in figure 6. The results taking into account the dielectric effect can be calculated from figure 6 using  $\epsilon_{\text{CdSe}} = 10.16$  [31], and equations (13) and (14). The effective-mass parameters are cited from Xia *et al* [30]. The splitting energies are  $\Delta_{\text{so}} = 418$  and  $\Delta_{\text{c}} = 40$  meV [31]. The



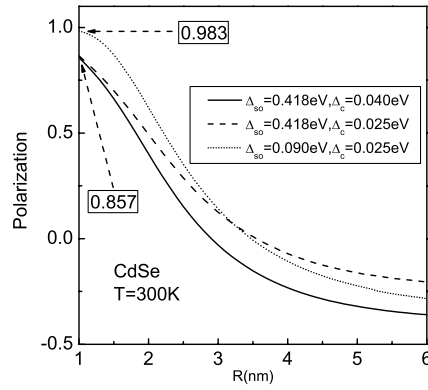


**Figure 6.** Calculated linear polarization factor of CdSe wurtzite quantum wires ignoring the dielectric effect as functions of  $R$ . We assume that the finite long wire can also be calculated approximately in our infinitely long wire model. We choose the length of wire  $L = 90$  nm and  $L/(2R) \geq 7.5$  so that the dielectric effect can be ignored (isotropic) [22], and the infinitely long wire model is also suitable. The solid line is the real case.

solid line is the real case. We see that the linear polarization factor is 0.857 at  $R = 1$  nm, in agreement with the experiment result [21]. This value is much smaller than unity, unlike 0.979 in the GaN case. We see that the splitting energies  $\Delta_c$  and  $\Delta_{so}$  of CdSe are both bigger than those of GaN. We will try to change the splitting energies of CdSe to find the factor which leads to the relatively small value of 0.857. At first we make the crystal field splitting energy  $\Delta_c$  of CdSe smaller, from 40 to 25 meV; the result is shown by the dashed line in figure 6. We see that, with smaller  $\Delta_c$ , the absolute value of the linear polarization factor at very large radius  $R$  (bigger than 5 nm, similar to the bulk material case) is smaller, and the linear polarization factor decreases more slowly with increasing  $R$ , but the value at  $R = 1$  nm changes little. Then we make the spin-orbit splitting energy  $\Delta_{so}$  of CdSe smaller, from 418 to 90 meV. The result is shown by the dotted line in figure 6. We see that, with smaller  $\Delta_{so}$ , compared with the dashed line, the absolute value of the linear polarization factor is bigger when  $R$  is very small or very large. And the linear polarization factor at  $R = 1$  nm is 0.983, much bigger than 0.857 in the real case, even bigger than 0.979 in the GaN case. So the relatively small linear polarization factor of CdSe wurtzite quantum wires with very small radius mainly stems from the big spin-orbit splitting energy  $\Delta_{so}$  of CdSe material with wurtzite structure.

#### 4. Conclusion

The electronic structure and optical properties of freestanding GaN wurtzite quantum wires are studied in the framework of six-band effective-mass envelope function theory. It is found that the electron states are either twofold or fourfold degenerate. There is a dark exciton effect when the radius  $R$  of GaN wurtzite quantum wires is in the range of [0.7, 10.9] nm. The linear polarization factors are calculated in three cases, the quantum confinement effect (finite long wire), the dielectric effect and both effects (infinitely long wire). It is found that the linear polarization factor of a finite long wire whose length is much less than the electromagnetic wavelength decreases as  $R$  increases, is very close to unity (0.979) at  $R = 1$  nm, and changes from a positive value to a negative value around  $R = 4.1$  nm. The linear polarization factor of the dielectric effect is 0.934, independent of radius, as long as the radius remains much less than the electromagnetic wavelength. The result for both effects shows that the quantum

confinement effect gives a correction to the dielectric effect result. It is found that the linear polarization factor of very long (treated approximately as infinitely long) quantum wires is in the range of [0.8,1]. The linear polarization factors of the quantum confinement effect of CdSe wurtzite quantum wires are calculated for comparison. The linear polarization factor of  $R = 1$  nm is 0.857, in agreement with the experimental results [21]. This value is much smaller than unity, unlike 0.979 in the GaN case, mainly due to the big spin-orbit splitting energy  $\Delta_{so}$  of CdSe material.

## Acknowledgments

This work is supported by the National Natural Science Foundation of China No. 90301007 and the special funds for Major State Basic Research Project No. G001CB3095 of China.

## References

- [1] Johnson J C, Choi H-J, Knutsen K P, Schaller R D, Yang P and Saykally R J 2002 *Nature* **1** 106
- [2] Duan X, Huang Yu, Agarwal R and Lieber C M 2003 *Nature* **421** 241
- [3] Yang P, Yan H, Mao S, Russo R, Johnson J, Saykally R, Morris N, Pham J, He R and Choi H-J 2002 *Adv. Funct. Mater.* **12** 323
- [4] Kim J-R, Oh H, So H M, Kim J-J, Kim J, Lee C J and Lyu S C 2002 *Nanotechnology* **13** 701
- [5] Liu C H, Zapfen J A, Yao Y, Meng X M, Lee C S, Fan S S, Lifshitz Y and Lee S T 2003 *Adv. Mater.* **15** 838
- [6] Kind H, Yan H, Messer B, Law M and Yang P 2002 *Adv. Mater.* **14** 158
- [7] Keem K, Kim H, Kim G-T, Lee J S, Min B, Cho K, Sung M-Y and Kim S 2004 *Appl. Phys. Lett.* **84** 4376
- [8] Mao C, Solis D J, Reiss B D, Kottmann S T, Sweeney R Y, Hayhurst A, Georgiou G, Iverson B and Belcher A M 2004 *Science* **303** 213
- [9] Banerjee S, Dan A and Chakravorty D 2002 *J. Mater. Sci.* **37** 4261
- [10] Law M, Goldberger J and Yang P 2004 *Annu. Rev. Mater. Res.* **34** 83
- [11] Shi W S, Zheng Y F, Wang N, Lee C S and Lee S T 2001 *Chem. Phys. Lett.* **345** 377
- [12] Peng H Y, Wang N, Zhou X T, Zheng Y F, Lee C S and Lee S T 2002 *Chem. Phys. Lett.* **359** 241
- [13] Han W, Fan S, Li Q and Hu Y 1997 *Science* **277** 1287
- [14] Peng H Y, Zhou X T, Wang N, Zheng Y F, Liao L S, Shi W S, Lee C S and Lee S T 2000 *Chem. Phys. Lett.* **327** 263
- [15] Park Y S, Park C M, Fu D J, Kang T W and Oh J E 2004 *Appl. Phys. Lett.* **85** 5718
- [16] Chen X, Xu J, Wang R M and Yu D 2003 *Adv. Mater.* **15** 419
- [17] Lian C X, Li X Y and Liu J 2004 *Semicond. Sci. Technol.* **19** 417
- [18] Han S, Jin W, Zhang D, Tang T, Li C, Liu X, Liu Z, Lei B and Zhou C 2004 *Chem. Phys. Lett.* **389** 176
- [19] Wang J, Gudiksen M S, Duan X, Cui Y and Lieber C M 2001 *Science* **293** 1455
- [20] Vouilloz F, Oberli D Y, Dupertuis M A, Gustafsson A, Reinhardt F and Kapon E 1998 *Phys. Rev. B* **57** 12378
- [21] Hu J, Li L-s, Yang W, Manna L, Wang L-w and Paul Alivisatos A 2001 *Science* **292** 2060
- [22] Ruda H E and Shik A 2005 *Phys. Rev. B* **72** 115308
- [23] McIntyre C R and Sham L J 1992 *Phys. Rev. B* **45** 9443
- [24] Li X-Z and Xia J-B 2002 *Phys. Rev. B* **66** 115316
- [25] Chichibu S F, Sota T, Cantwell G, Ason E D B and Litton C W 2003 *J. Appl. Phys.* **93** 756
- [26] Xia J B 1996 *J. Lumin.* **70** 120
- [27] Xia J-B, Cheah K W, Wang X-L, Sun D-Z and Kong M-Y 1999 *Phys. Rev. B* **59** 10119
- [28] *Landolt-Bornstein*, Group III, vol 41 A1b
- [29] Wang J, Gudiksen M S, Duan X, Cui Y and Lieber C M 2001 *Science* **293** 1455
- [30] Xia J-B and Li J 1999 *Phys. Rev. B* **60** 11540
- [31] *Landolt-Bornstein*, Group III, vol 17 B